

Synthesis and Molecular Structures of Some New Titanium(IV) Aryloxides

Karine Gigant, Adel Rammal, and Marc Henry*

Contribution from the Laboratoire de Chimie Moléculaire de l'État Solide, Université Louis Pasteur, Institut le Bel, 4, Rue Blaise Pascal, 67070 Strasbourg Cedex, France

Received August 24, 2001

Abstract: The coordination chemistry of model phenolic ligands (pyrocatechol, salicylic acid, and 2,2'-biphenol) that are able to form respectively five-, six-, or seven-membered rings with titanium(IV) alkoxides is investigated. With pyrocatechol, a polynuclear complex containing 10 Ti atoms was characterized with a not very common doubly bridging μ_3 -(O,O',O') coordination mode. With salicylic acid, a monomeric tris(chelate) complex was obtained. With 2,2'-biphenol, a polynuclear complex containing six Ti atoms was obtained showing both μ_2 -(O,O') and μ_2 -(O,O,O') coordination modes for the ligands. Intermolecular interactions in the solid state for these three new compounds are also quantitatively discussed using the partial charge model.

Introduction

Transition metal aryloxides are known to play a fundamental role in many areas. In biology, catechol functional groups are found in certain siderophores,¹ while polyphenols forms the basis of anthocyanins, the natural pigments that are responsible for most of the wide variety of colors displayed by flowers and fruits.² In catalysis, titanium aryloxides are widely used as precursors for homogeneous α -olefin polymerization catalysts³ or as asymmetric catalysts for enantioselective carbon–carbon bond-forming reactions.⁴ They are also involved in strong metal–support interactions in heterogeneous catalytic systems.⁵ In host–guest chemistry, titanium aryloxides are able to form interesting metallocalix[3,4]arenes structures.⁶ In coordination chemistry, catechol ligands are able to stabilize unusual coordination polyhedra,⁷ and this allows a good tuning of electrochemical properties.⁸ In supramolecular chemistry, titanium catecholates are known to self-assemble into helicate coordination compounds⁹ and were recently used for the rational design of high-symmetry coordination clusters through self-assembly reactions.¹⁰ Finally, quite recently, titanium aryloxide

bonds have been used to obtain covalent 3- and 2-D metal–organic frameworks.¹¹ Consequently, there is considerable interest in designing and synthesizing new titanium aryloxides. In this paper we report on the synthesis of three new titanium aryloxide compounds obtained by reacting titanium alkoxides with pyrocatechol (1,2-dihydroxybenzene), salicylic acid (*o*-hydroxybenzoic acid), and 2,2'-biphenol. Titanium alkoxides were selected owing to their ability to form, upon hydrolysis, titanium oxide-based nanocrystals.¹² Accordingly, TiO₂ is an attractive material because it is cheap, nontoxic, and highly insoluble in water, and because it displays interesting semiconducting properties. This allows TiO₂-based nanoparticles to be used in a wide range of processes with minimal environmental impact. Another motivation for this study was to check our ability to quantify molecular interactions in the crystalline state using a point charge approximation of DFT equations (partial charge model), as demonstrated in a previous communication.^{6d}

Pyrocatechol-Based Complexes

Pyrocatechol was selected because only two anionic titanium catecholates, [Et₃NH]₂[Ti(O₂C₆H₄)₃] and K₄[TiO(O₂C₆H₄)₂]·9H₂O, have been structurally characterized.¹³ In particular, no

(1) Raymond, K. N.; Carrano, C. J. *Acc. Chem. Res.* **1979**, *12*, 183–190.

(2) Elhabiri, M.; Figueiredo, P.; Toki, K.; Saito, N.; Brouillard, R. *J. Chem. Soc., Perkin Trans. 2* **1997**, 355–362.

(3) Firth, A. V.; Stewart, J. C.; Hoskin, A. J.; Stephan, D. W. *J. Organomet. Chem.* **1999**, *591*, 185–193. Okuda, J.; Fokken, S.; Kleinhenn, T.; Spaniol, T. P. *Eur. J. Inorg. Chem.* **2000**, 1321–1326.

(4) Eilerts, N. W.; Heppert, J. A.; Kennedy, M. L.; Takusagawa, F. *Inorg. Chem.* **1994**, *33*, 4813–4814. Terada, M.; Matsumoto, Y.; Nakamura, Y.; Mikami, K. *Inorg. Chim. Acta* **1999**, *296*, 267–272. Coles, S. J.; Hursthouse, M. B.; Kelly, D. G.; Toner, A. J.; Walker, N. M. *Can. J. Chem.* **1999**, *77*, 2095–2098.

(5) Toth, R. T.; Stephan, D. W. *Can. J. Chem.* **1991**, *69*, 172–178.

(6) (a) Hampton, P. D.; Daitch, C. E.; Alam, T. M.; Bencze, Z.; Rosay, M. *Inorg. Chem.* **1994**, *33*, 4750–4758. (b) Clegg, W.; Elsegood, M. R. J.; Teat, S. J.; Redshaw, C.; Gibson, V. C. *J. Chem. Soc., Dalton Trans.* **1998**, 3037–3039. (c) Zanotti-Gerosa, A.; Solari, E.; Giannini, L.; Floriani, C.; Re, N.; Chiesi-Villa, A.; Rizzoli C. *Inorg. Chim. Acta* **1998**, *270*, 298–311. (d) Rammal, A.; Brisach, F.; Henry, M. *J. Am. Chem. Soc.* **2001**, *123*, 5612–5613.

(7) Karpishin, T. B.; Stack, T. D. P.; Raymond, K. N. *J. Am. Chem. Soc.* **1993**, *115*, 182–192.

(8) Hahn, F. E.; Rupperecht, S.; Moock, K. H. *J. Chem. Soc., Chem. Commun.* **1991**, 224–225.

(9) Albrecht, M.; Kotila, S. *Angew. Chem., Int. Ed. Engl.* **1995**, *34*, 2134–2137. Albrecht, M.; Röttele, H.; Burger, P. *Chem. Eur. J.* **1996**, *2*, 1264–1268. Albrecht, M.; Schneider, M.; Fröhlich, R. *New J. Chem.* **1998**, 753–754.

(10) Brückner, C.; Powers, R. E.; Raymond, K. N. *Angew. Chem., Int. Ed.* **1998**, *37*, 1837–1839. Scherer, M.; Caulder, D. L.; Johnson, D. W.; Raymond, K. N. *Angew. Chem., Int. Ed.* **1999**, *38*, 1588–1592.

(11) (a) Vaid, T. P.; Lobkovsky, E. B.; Wolczanski, P. T. *J. Am. Chem. Soc.* **1997**, *119*, 8742–8743. (b) Vaid, T. P.; Tanski, J. M.; Pette, J. M.; Lobkovsky, E. B.; Wolczanski, P. T. *Inorg. Chem.* **1999**, *38*, 3394–3405. (c) Tanski, J. M.; Lobkovsky, E. B.; Wolczanski, P. T. *Solid State Chem.* **2000**, *152*, 130–140. (d) Tanski, J. M.; Vaid, T. P.; Lobkovsky, E. B.; Wolczanski, P. T. *Inorg. Chem.* **2000**, *39*, 4756–4765. (e) Tanski, J. M.; Wolczanski, P. T. *Inorg. Chem.* **2001**, *40*, 2026–2033.

(12) Moritz, T.; Reiss, J.; Diesner, K.; Su, D.; Chemseddine, A. *J. Phys. Chem. B* **1997**, *101*, 8052–8053. Chemseddine, A.; Moritz, T. *Eur. J. Inorg. Chem.* **1999**, 235–245. Elder, S. H.; Cot, F. M.; Su, Y.; Heald, S. M.; Tyryshkin, A. M.; Bowman, M. K.; Gao, Y.; Joly, A. G.; Balmer, M. L.; Kolwaite, A. C.; Magini, K. A.; Blake, D. M. *J. Am. Chem. Soc.* **2000**, *122*, 5138–5146.

(13) Borgias, B. A.; Cooper, S. R.; Koh, Y. B.; Raymond, K. N. *Inorg. Chem.* **1984**, *23*, 1009–1016.

neutral complexes involving only titanium atoms and pyrocatechol ligands have been isolated so far as single crystals. Although a molecular complex, $[\text{Ti}_6\text{O}_4(\text{OPr}^i)_4(\text{O}_2\text{C}_6\text{H}_4)_4\{(\text{CO})_9\text{Co}_3\text{CCO}_2\}_4]$, has been reported,¹⁴ it was a bimetallic compound displaying bridging carboxylic groups. Furthermore, pyrocatechol was selected because of the ability of its two isomers, resorcinol (1,3-dihydroxybenzene)^{11c} and hydroquinone (1,4-dihydroxybenzene),^{11a,b} to form titanium-based 3-D covalent metal–organic network. Obviously, the spatial disposition of the two hydroxyl groups in pyrocatechol should favor chelation over bridge formation.

In agreement with literature,¹⁴ attempts to obtain single crystals for molar ratios $R = \text{pyrocatechol/Ti}$ higher than 1 were unsuccessful. On the other hand, limpid red-orange-colored solutions could be obtained by mixing $\text{Ti}(\text{OBU}^n)_4$ or $\text{Ti}(\text{OPr}^i)_4$ alkoxides with pyrocatechol with $R \leq 1$. However, under anhydrous conditions, no precipitation occurs, even after several months of aging. Upon addition of a small amount of water to these limpid solutions, crystalline materials could be obtained for $h = \text{H}_2\text{O/Ti} < 0.5$, while amorphous precipitates are formed for $h > 2$. After several trials, it was found that the highest yields of microcrystalline precipitates were observed for $h = 0.3$ and $R = 0.75$ with $\text{Ti}(\text{OBU}^n)_4$ (**1**) and for $h = 0.4$ and $R = 0.8$ with $\text{Ti}(\text{OPr}^i)_4$ (**2**). Recrystallization of **1** by slow diffusion in 1-butanol afforded platelet crystals suitable for X-ray diffraction.¹⁵

As shown in Figure 1a, the overall stoichiometry of **1** is $\text{Ti}_5\text{O}_{18}\text{C}_{52}\text{H}_{79}$, which may be formulated as $[\text{Ti}_{10}\text{O}_6(\text{OBU}^n)_{12}(\text{HOBU}^n)_2(\text{pc})_8]$ (pc = pyrocatechol). Its molecular structure can be described as two tetrahedral ($\mu_4\text{-O}$) Ti_4 building blocks sharing corners with one central edge-sharing dioctahedral unit and leading to a bowtie-shaped molecule. Interestingly, a rather similar but isolated tetrahedral ($\mu_4\text{-O}$) Ti_4 unit was reported in the crystal structure of $[\text{Ti}_4\text{O}_2(\text{OR})_{10}(\text{O}_2\text{CH}_2)_2]$.¹⁶ If the tetrahedral units are found to be much less regular ($d_{\text{Ti-O}} = 199, 204, 209,$ and 222 pm in the present case), they display however the same characteristic, i.e., butterfly-shaped distortion (five O–Ti–O bond angles at $102 \pm 1^\circ$ and one at 143°). TiO_6 octahedra (average $d_{\text{Ti-O}} = 197$ pm) are also found to be considerably distorted ($175 \text{ pm} < d_{\text{Ti-O}} < 222$ pm, average $\theta_{\text{O-Ti-O}} = 104^\circ$) and appear to be linked together through three pyrocatechol and two butoxy ligands. As previously observed,¹⁴ for each pyrocatechol ligand, one of its oxygen atoms bridges two Ti centers ($\theta_{\text{Ti-O-Ti}} = 105^\circ (\times 2), 108^\circ$), whereas the other one coordinates a titanium atom in a terminal fashion (chelating-bridging coordination mode, Figure 1b). However, a significant increase in the Ti–O–Ti bond angles from 99° ¹⁴ is observed. Similarly, if the Ti–O distances for the terminal O atom are found to be rather similar ($d_{\text{Ti-O}} = 187\text{--}188$ pm here versus 187 pm¹⁴), a considerable spreading for the bridging O atom ($d_{\text{Ti-O}} = 198, 212, 217$ pm here versus 219 pm¹⁴) is observed. Concerning the butoxy groups, we may refer to the crystal structure of

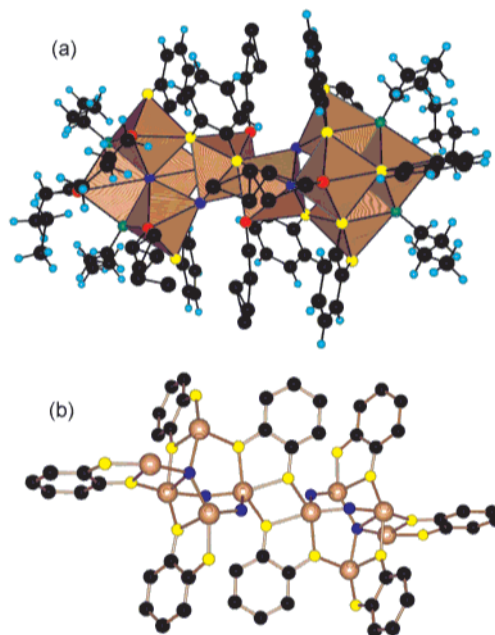


Figure 1. Molecular structure of **1**. (a) Bowtie shape of $[\text{Ti}_{10}\text{O}_6(\text{OBU}^n)_{12}(\text{HOBU}^n)_2(\text{pc})_8]$ (pc = pyrocatechol). Among the 12 butoxy groups, 4 are found in the bridging position (green O atoms) and 8 in the terminal position (red O atoms). (b) The two coordination modes around the titanium oxo core (blue O atoms) of the eight pyrocatechol ligands (yellow O atoms).

$[\text{Ti}_6\text{O}_4(\text{OBU}^n)_{10}(\text{O}_2\text{CCH}_3)_8]$ displaying similar bridging ($d_{\text{Ti-O}} = 196$ and 206 pm) and terminal ($d_{\text{Ti-O}} = 174\text{--}177$ pm) butoxy groups.¹⁷ In the present case of the two $\mu_2\text{-OBU}^n$ bridges, one appears to be much more symmetric ($d_{\text{Ti-O}} = 197$ and 200 pm) than the other ($d_{\text{Ti-O}} = 196$ and 206 pm), and no significant differences are observed for the four terminal OBU^n ligands ($d_{\text{Ti-O}} = 174\text{--}177$ pm). However, the two butoxy group linked to the two Ti atoms bearing $\mu_2\text{-oxo}$ ligands are found to be disordered. The most interesting features are displayed by the central dioctahedral unit $[(\mu_2\text{-O})_2(\text{HOBU}^n)\text{Ti}\{(\mu_2\text{-O})\text{C}_6\text{H}_4(\mu_2\text{-O})\}_2\text{Ti}(\text{HOBU}^n)(\mu_2\text{-O})_2]$. To the best of our knowledge, this is the first structural characterization of a Ti–HOBUⁿ solvate bond. As protons have not been localized during the crystal structure determination, the reported X-ray stoichiometry was $[\text{Ti}_{10}\text{O}_6(\text{OBU}^n)_{14}(\text{pc})_8]^{2-}$, showing that two protons were missing. An easy localization of these protons was, however, possible through the use of the bond valence sum (BVS) technique.¹⁸ Accordingly, BVS values close to 2 were found for all O atoms except for atom O17 (BVS = 1.2). This rather low value together with a rather long Ti–O bond length (222 pm) suggested missing atoms around this center. The simplest way to restore the balance is to assume that the OBU^n group is, indeed, a butanol molecule directly bonded to Ti atoms. The disorder observed on this molecule would then be a direct consequence of a rather weak solvate bond. A strong nonequivalence is also observed between the inner-bridging pyrocatecholato ligand ($d_{\text{Ti-O}} = 199\text{--}210$ pm, $\theta_{\text{Ti-O-Ti}} = 104^\circ$) and the outer-bridging one ($d_{\text{Ti-O}} = 205\text{--}210$ pm, $\theta_{\text{Ti-O-Ti}} = 122^\circ$). Finally, the four $\mu_2\text{-oxo}$ bridges linking the central dioctahedral unit to the two peripheral butterfly-shaped OTi_4 units are characterized by $d_{\text{Ti-O}} = 177\text{--}187$ pm ($\theta_{\text{Ti-O-Ti}} = 133^\circ$) and $d_{\text{Ti-O}} = 179\text{--}189$ pm ($\theta_{\text{Ti-O-Ti}} = 134^\circ$). As evidenced by ¹H NMR, this solid-state structure is also conserved in solution, with no chemical exchange between

(14) Lei, X.; Shang, M.; Fehlnner, T. P. *Organometallics* **1996**, *15*, 3779–3781. Lei, X.; Shang, M.; Fehlnner, T. P. *Organometallics* **1997**, *16*, 5289–5301.

(15) Crystal data for **1**: $\text{C}_{52}\text{H}_{79}\text{O}_{18}\text{Ti}_5$, $M_r = 1231.70$, monoclinic, space group $P2_1/c$, $a = 13.3800(4)$ Å, $b = 32.335(1)$ Å, $c = 14.2883(3)$ Å, $\beta = 106.740(2)^\circ$, $V = 5919.8(5)$ Å³, $Z = 4$, $\rho_{\text{calcd}} = 1.38$ g·cm⁻³, MoK α radiation (graphite monochromator), $\mu = 0.712$ mm⁻¹, 31151 intensity data collected at 173 K, 15830 unique, no absorption correction. The structure was solved using direct methods and refined against $|F|$ [7549 reflections having $I > 3\sigma(I)$]. Hydrogen atoms were introduced as fixed contributors when a residual electronic density was observed near their expected positions. For all computations the Nonius OpenMoleN package was used. Refinement converged at $R_1 = 0.059$, $wR_2 = 0.086$, final GOF = 1.388. Residual electron density was in the range $-0.222, 0.775$ e·Å⁻¹.

(16) Boyle, T. J.; Alam, T. M.; Tafuya, C. J.; Scott, B. L. *Inorg. Chem.* **1998**, *37*, 5588–5594.

(17) Doeuff, S.; Dromzee, Y.; Taulelle, F.; Sanchez, C. *Inorg. Chem.* **1989**, *28*, 4439.

(18) Brown, I. D.; Altermatt, D. *Acta Crystallogr.* **1985**, *B41*, 244–247.

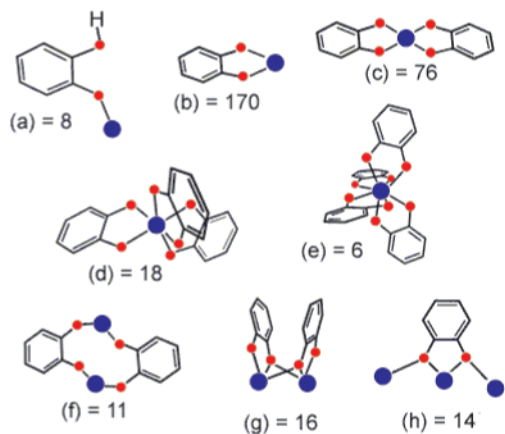


Figure 2. Coordination modes of the pyrocatecholato ligand characterized through single-crystal X-ray diffraction. The number after the letter is the occurrence found in the 5.21 release of the Cambridge Crystallographic Database. Metal and oxygen atoms in blue and red, respectively. (a) Monodentate mode. (b–e) Chelate modes (mono, bis, tris, and tetrakis). (f) Singly bridging μ_2 -(O,O') mode. (g) Singly bridging chelate μ_2 -(O,O',O') mode. (h) Doubly bridging chelate μ_3 -(O,O',O,O') mode.

pyrocatechol ligands. However, it is readily hydrolyzed since we have not been able to record ^{13}C or ^{17}O NMR spectra. Interestingly, ^{17}O NMR shows that upon hydrolysis, the μ_4 -oxo group is transformed into a μ_3 -oxo entity while the μ_2 -oxo groups remain observable. As we have in hand the chemical proof that pyrocatechol ligands are able to link with Ti atoms using a doubly bridging μ_3 -(O,O,O',O') coordination mode, the fact that we have been unable to obtain crystalline materials for $R \geq 1$ may be readily explained. As catechol molecules behave as truly trifunctional units, one may expect reticulated insoluble polymers rather than soluble molecular species (chelation or μ_2 -coordination mode) for species such as $\text{Ti}(\text{OR})_2$ -(pc) or $\text{Ti}(\text{pc})_2$. At this stage, it may be interesting to review the currently known coordination modes of pyrocatechol derivatives.

As shown in Figure 2, among the 319 hits in the 5.21 release (January 2001) of the Cambridge Crystallographic Database, 85% reveal a chelating coordination mode (Figure 2b–e) with a wide range of elements. The occurrences of the μ_2 -(O,O',O') (Figure 2g) and μ_3 -(O,O',O,O') (Figure 2h) evidenced in **1** are 5% and 4%, respectively, and only two recent papers have reported the existence of homonuclear trimetallic μ_3 -(O,O',O,O') bridges with $\text{Zr}^{19\text{a}}$ and Mn, Fe, and $\text{Zn}^{19\text{b}}$ centers. It is our feeling that this type of bridge should, in fact, be quite common but that the insolubility of the resulting polymeric materials prevents their accurate structural characterization. It is also worth noticing that although the bridging modes identified for hydroquinone (hq) in $[\text{Ti}(\text{hq})_2]^{11\text{a,b}}$ and resorcinol (res) in $[\text{Ti}(\text{res})(\text{resH})_2]^{11\text{c}}$ are rather similar, μ_2 -(O,O), μ_2 -(O,O'), and μ_3 -(O,O,O'), they are completely different from those identified here. Quite different geometries are then expected for $[\text{Ti}(\text{pc})_2]$ networks. Finally, let us notice that **1** displays an interesting layered structure in the solid state based on a planar four-connected net (Figure 3).

Applying the partial charge model^{6d} to this molecular net ($Z = 2$) leads to an electrostatic balance $\text{EB}_{\text{net}} = -65358.9 \text{ kJ}\cdot\text{mol}^{-1}$, which should be compared to the electrostatic balance of a free complex $[\text{Ti}_{10}\text{O}_6(\text{OBU}^{\text{n}})_{12}(\text{HOBu}^{\text{n}})_2(\text{pc})_8]$, $\text{EB}_{\text{mol}} =$

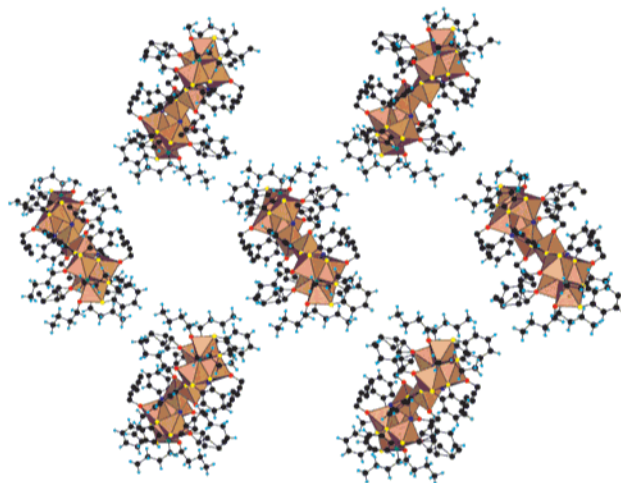


Figure 3. Planar four-connected van der Waals net formed by **1** in the solid state.

$-32678.1 \text{ kJ}\cdot\text{mol}^{-1}$. This points to a rather low lattice energy: $E_{\text{lattice}} = \text{EB}_{\text{net}} - 2\text{EB}_{\text{mol}} = -2.7 \text{ kJ}\cdot\text{mol}^{-1}$, typical of rather weak van der Waals interactions. This clearly shows that for a network built from similar neutral building blocks, there is almost no residual energy associated with the stacking process.

Salicylic Acid Complexes

Having established the possible coordination modes between pyrocatechol ligands and Ti atoms, our next step was to investigate the effect of substituting one of the two OH groups by a carboxylic group. Since titanium oxocarboxylates are widely used in sol–gel chemistry,²⁰ we were interested in studying mixed phenolic–carboxylic complexes. Figure 4 shows the 13 known coordination modes of salicylic acid with a metallic center, compiled after a survey of the 5.21 release of the Cambridge Crystallographic Database. The only hit for Ti(IV) was a molecular complex, $[\text{Ti}_6\text{O}_6(\text{OEt})_6(\text{O}_2\text{C}_6\text{H}_4\text{OPh})_6]$; however, it is rather remote with respect to our study, as the hydroxyl moiety was protected by a phenyl group.²¹ A comparison between Figures 2 and 4 shows the dramatic increase in the possible coordination modes (from 5 to 13) induced by the $\text{OH} \rightarrow \text{COOH}$ substitution. Major coordination modes are found to be chelating (O,O') or O-terminal (27% both), μ_2 -(O',O'') bridging (17%), chelating (O',O'') (13%), and μ_2 -(O,O',O'') bridging (5%). Network-forming coordination modes (μ_3 and higher) are known but are not common (7%).

It was then hoped that upon reaction of titanium alkoxides with salicylic acid, molecular species could be formed. Accordingly, several crystalline phases were readily obtained by varying the ratio $R = [\text{salH}_2]/[\text{Ti}(\text{OBU}^{\text{n}})_4]$ between 0.5 and 5 and the hydrolysis ratio $H = [\text{H}_2\text{O}]/[\text{Ti}]$ between 0 and 1. However, owing to their rather small sizes, most of these crystals were unsuitable for X-ray diffraction. The only case in which we have been able to get red-orange cubic single crystals suitable for X-ray diffraction²² was for $H = 0$ and $R = 5$. Owing to the rather high R value, we were not surprised to obtain the Ti(IV) monomeric octahedral complex (**3**) (Figure 5) with the stoichiometry $\text{TiO}_{11}\text{C}_{29}\text{H}_{34}$. To the best of our knowledge, this is the first report of a tris(salicylato) complex of a transition metal. The crystal is built from 1-butanol-solvated van der Waals

(20) Rammal, A.; Brisach, F.; Henry, M. C. *R. Acad. Sci., Ser. IIc (Chem.)*, in press.

(21) Papiernik, R.; Hubert-Pfalzgraf, L. G.; Vaissermann, J.; Goncalves, M. C. H. B. *J. Chem. Soc., Dalton Trans.* **1998**, 2285–2287.

(19) (a) Chi, Y.; Lan, J. W.; Ching, W. L.; Peng, S. M.; Lee, G. H. *J. Chem. Soc., Dalton Trans.* **2000**, 2923–2927. (b) Reynolds, R. A., III; Coucouvanis, D. *Inorg. Chem.* **1998**, 37, 170–171.

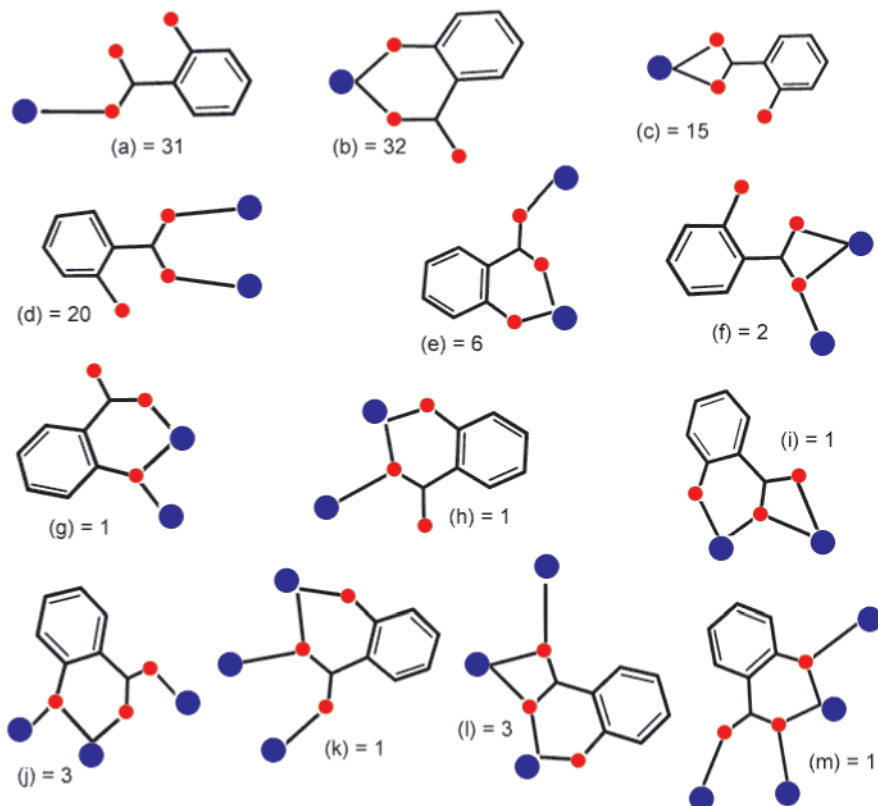


Figure 4. Coordination modes of the salicylato ligand characterized through single-crystal X-ray diffraction. The number after the letter is the occurrence found in the 5.21 release of the Cambridge Crystallographic Database. Metal and oxygen atoms in blue and red, respectively. (a) Monodentate mode. (b) Chelate (O,O') mode. (c) Chelate (O',O'') mode. (d) Bridging μ_2 -(O',O'') mode. (e) Bridging chelate μ_2 -(O,O',O''). (f) Bridging chelate μ_2 -(O',O',O''). (g) Bridging chelate μ_2 -(O,O,O'). (h) Bridging chelate μ_2 -(O,O',O''). (i) Bridging chelate μ_2 -(O,O',O',O''). (j) Doubly bridging chelate μ_3 -(O,O,O',O''). (k) Doubly bridging chelate μ_3 -(O,O',O',O''). (l) Doubly bridging chelate μ_3 -(O,O',O',O'',O''). (m) Triply bridging chelate μ_3 -(O,O,O',O',O'').

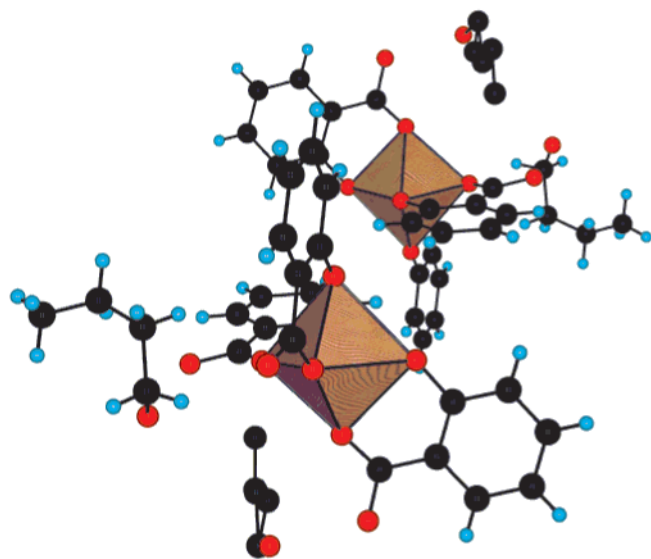


Figure 5. Molecular structure of the (Λ,Δ) -[Ti(sal)(salH)₂](ⁿBuOH)₂ dimer found in the crystal structure of **3**.

dimers and may be formulated (Λ,Δ) -[Ti(sal)(salH)₂](ⁿBuOH)₂, with sal = *o*-O₂CC₆H₄O.

The occurrence of two (*o*-carboxylato)phenolato ligands (salH) within the titanium coordination sphere was suggested by the observation of one normal ($d_{C-O} = 125 \text{ pm} < d_{C-O_{Ti}} = 128 \text{ pm}$) and two inverse ($d_{C-O_{1,08}} = 130 \text{ pm} > d_{C-O_{Ti}} = 125 \text{ pm}$) coordination modes for the carboxylic group. Assuming that the shortest bond corresponds to the carbonyl group, these

data suggest a Ti—O—(C=O) configuration for one salicylato ligand and a Ti—(O=C)—OH configuration for the two other one (salH forms). This interesting geometry is fully coherent with the occurrence of two very short O...O distances ($d_{O8-O10} = 250 \text{ pm}$ and $d_{O1-O11} = 255 \text{ pm}$) if atoms O1 and O8 are assumed to be OH groups of the salH ligand (O10 and O11 belong to butanol molecules). The presence of the two butanol molecules in the unit cell may be readily explained by the existence of two strong hydrogen bonds, salH...HOBuⁿ. The nonequivalence of these two butanol molecules is further evidenced by the fact that the butoxy fragment linked to atom O11 is disordered, which may well be a direct consequence of weaker interactions (longer O...O bond) with one salH ligand. ¹H and ¹³C NMR showed that the tris-chelate structure is perfectly stable in solution, with no differentiation between sal and salH ligands on the NMR time scale. Work is currently in progress in order to grow larger single crystals for the other crystalline materials obtained in this system.

Another interesting point of this structure is the possibility of evaluating the average strength of the hydrogen-bonding

(22) Crystal data for **3**: C₂₉H₃₄O₁₁Ti, $M_r = 606.49$, monoclinic, space group $P2_1/n$, $a = 14.2660(4) \text{ \AA}$, $b = 13.2240(7) \text{ \AA}$, $c = 15.8470(7) \text{ \AA}$, $\beta = 100.699(3)^\circ$, $V = 2937.6(4) \text{ \AA}^3$, $Z = 4$, $\rho_{\text{calcd}} = 1.37 \text{ g}\cdot\text{cm}^{-3}$, MoK α radiation (graphite monochromator), $\mu = 0.350 \text{ mm}^{-1}$, 17890 intensity data collected at 173 K, 8612 unique, no absorption correction. The structure was solved using direct methods and refined against $|F|$ [5140 reflections having $I > 3\sigma(I)$]. Hydrogen atoms were introduced as fixed contributors when a residual electronic density was observed near their expected positions. Hydrogen atoms were not assigned for disordered solvent molecules. For all computations the Nonius OpenMoleN package was used. Refinement converged at $R_1 = 0.062$, $wR_2 = 0.081$, final GOF = 1.548. Residual electron density was in the range $-0.120, 0.681 \text{ e}\cdot\text{\AA}^{-1}$.

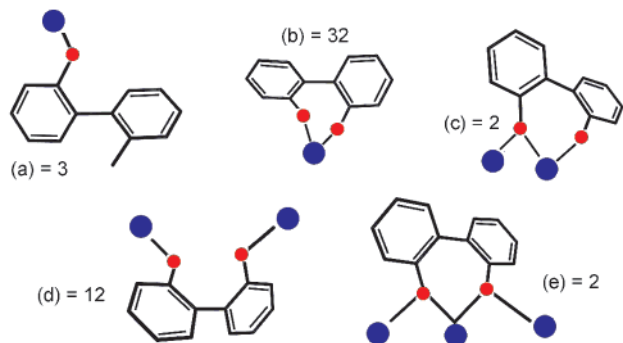


Figure 6. Coordination modes of the 2,2'-biphenolato ligand characterized through single-crystal X-ray diffraction. The number after the letter is the occurrence found in the 5.21 release of the Cambridge Crystallographic Database. Metal and oxygen atoms in blue and red, respectively. (a) Monodentate mode. (b) Chelate (O,O') mode. (c) Bridging chelate (O,O,O') mode. (d) Bridging μ_2 -(O,O') mode. (e) Doubly bridging chelate μ_3 -(O,O,O',O') mode.

pattern using the partial charge model.^{6d} First, the isolated dimer (Λ, Δ)-[Ti(sal)(salH)₂](^tBuOH)₂ is characterized by $EB_{\text{dim}} = -11225.5 \text{ kJ}\cdot\text{mol}^{-1}$, while for the isolated fragments we found $EB_{\text{monol}}[\text{Ti}(\text{sal})(\text{salH})_2] = -5200.3 \text{ kJ}\cdot\text{mol}^{-1}$ (total charge $Q = -0.25$), $EB_{\text{BuOH}\#1} = -124.7 \text{ kJ}\cdot\text{mol}^{-1}$ ($Q = +0.09$), and $EB_{\text{BuOH}\#2} = -150.4 \text{ kJ}\cdot\text{mol}^{-1}$ ($Q = +0.15$). The total hydrogen bond energy should then be $E_{\text{tot}} = 2(E_{\text{mono}} + EB_{\text{BuOH}\#1} + EB_{\text{BuOH}\#2}) - EB_{\text{dim}} = -274.7 \text{ kJ}\cdot\text{mol}^{-1}$. With a total of eight hydrogen bonds per dimer, the average strength is then found to be $E_{\text{HB}} = E_{\text{tot}}/8 = -34 \text{ kJ}\cdot\text{mol}^{-1}$, i.e. about 2 times the hydrogen bond energy in hexagonal ice ($\sim 18 \text{ kJ}\cdot\text{mol}^{-1}$) for which the O...O bond length is substantially longer (275 pm). On the other hand, applying our method to the simple hexagonal ice network leads to $E_{\text{HB}} = (-850.5/4 + 179.1)/2 = -16.8 \text{ kJ}\cdot\text{mol}^{-1}$. These data clearly demonstrate our ability to handle the hydrogen bond on a quantitative basis with an estimated error of about 10%.

2,2'-Biphenol Complexes

Our last concern will be the characterization of molecular titanium(IV) complexes involving 2,2'-biphenol as a ligand. The latter was used to check the effect of increasing ring size in the chelation sequence pyrocatechol (five-membered rings) \rightarrow salicylic acid (six-membered rings) \rightarrow 2,2'-biphenol (seven-membered rings). As shown in Figure 6, the preferred coordination modes for 2,2'-biphenol are chelating (62%) or μ_2 -bridging (23%). As no complex between Ti(IV) and 2,2'-biphenol has yet been isolated, it was interesting to see what coordination mode could be observed. The selection of this particular molecule was also interesting with respect to the formation of a titanium-based 3-D covalent metal-organic network with the closely related 4,4'-biphenol ligand.^{11c} Obviously, the spatial disposition of the two hydroxyl groups in 2,2'-biphenol should favor molecular species over reticulated networks. Interestingly, weakly soluble orange crystalline materials were rapidly obtained upon reaction of titanium isopropoxide and 2,2'-biphenol at $R = 2$ and $H = 0$ (compound **4**). Recrystallization of a chloroform solution of **4** by slow diffusion in 2-propanol afforded orange platelike crystals suitable for X-ray diffraction and showing the $\text{Ti}_6\text{O}_{22}\text{C}_{92}\text{H}_{92}\text{Cl}_6$ stoichiometry.²³ The observation of a quasi planar ladder-like Ti_6O_4 exameric core (Figure 7) based on four μ_3 -oxo groups ($192 \text{ pm} \leq d_{\text{Ti}-\text{O}} \leq 206 \text{ pm}$) is the main feature of this molecular structure.

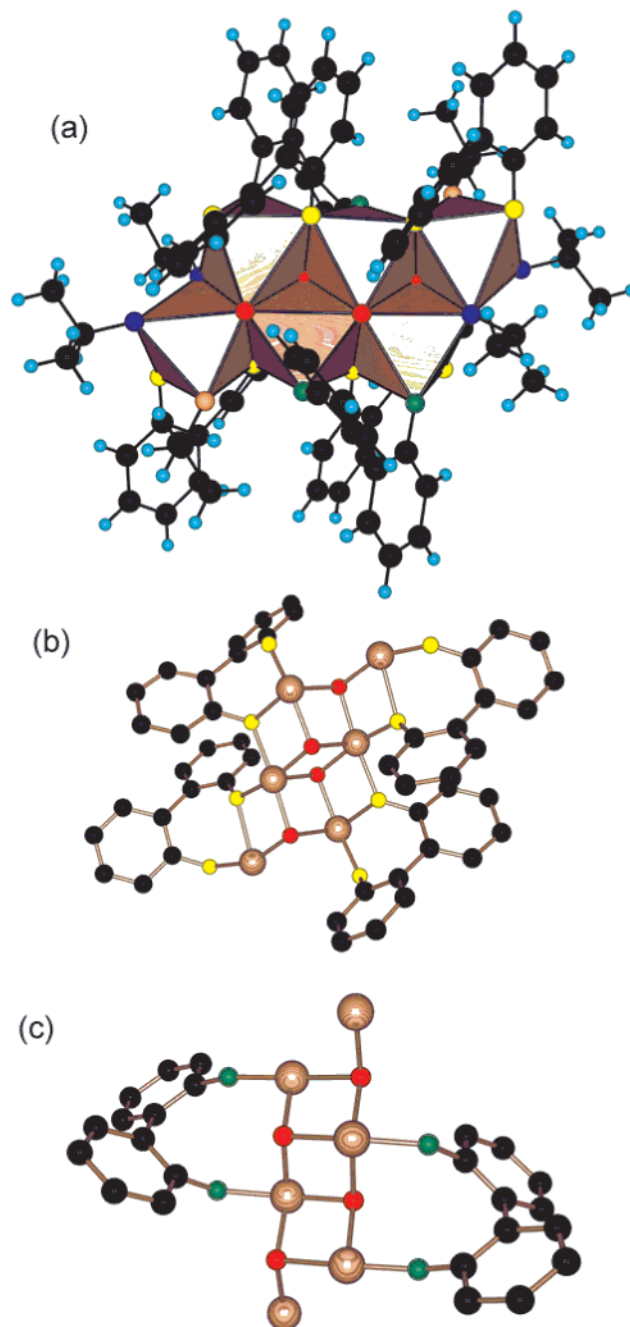


Figure 7. Molecular structure of **4**. (a) Planar hexamer $[\text{Ti}_6\text{O}_4(\text{OPr})_4(\text{HOPr})_2(\text{bph})_6]$ ($\text{bph} = 2,2'$ -biphenol). Among the four isopropoxy groups, two are found in the bridging position and two in the terminal position (blue O atoms). Brown O atoms corresponds to the two 2-propanol molecules. (b) The bridging chelating coordination mode displayed by four 2,2'-biphenolato ligands (yellow O atoms). (c) The Ti_6O_4 ladder core (red O atom) and the bridging coordination mode of the remaining two 2,2'-biphenolato ligands (green O atoms).

If titanium-oxygen ladders were already observed previously with calix[4]arene ligands,²⁴ they were limited to tetramers. Here we observe the possibility of forming a higher nuclearity complex. For this complex, one could identify two bridging ($d_{\text{Ti}-\text{O}} = 198, 201 \text{ pm}$) isopropoxy groups, two terminal isopropoxy groups ($d_{\text{Ti}-\text{O}} = 178 \text{ pm}$), two coordinated 2-propanol molecules ($d_{\text{Ti}-\text{O}} = 213 \text{ pm}$), two μ_2 -(O,O') bridging 2,2'-biphenol (bph) groups ($d_{\text{Ti}-\text{O}} = 181, 190 \text{ pm}$), and four μ_2 -(O,O,O') chelating-bridging bph groups ($d_{\text{Ti}-\text{O}} = 185, 197, 222 \text{ pm}$, $\theta_{\text{Ti}-\text{O}-\text{Ti}} = 96^\circ$ for the two outer bph ligands and $d_{\text{Ti}-\text{O}} =$

184, 203, 210 pm, $\theta_{\text{Ti-O-Ti}} = 98^\circ$ for the two inner ones). Dihedral angles between aromatic planes were found to be 60° for $\mu_2\text{-(O,O')-bph}$, 49° for outer $\mu_2\text{-(O,O,O')-bph}$, and 46° for inner $\mu_2\text{-(O,O,O')-bph}$. It is worth noting that, although the $\mu_2\text{-(O,O,O')-bph}$ bridge has been characterized for transition metals such as iron^{25a} or manganese,^{25b} the case reported here represents the first occurrence of a $\mu_2\text{-(O,O')-bph}$ bridge with an atom other than P(V). The presence of a 2-propanol molecule in the structure was deduced from the calculation of -2 charge excess from the X-ray stoichiometry. The observation of a bond valence sum of only 1.3 around atom O9, versus values in the range from 1.9 to 2.2 for all other O atoms, points to the localization of the two missing protons. Moreover, the short bond distance (267 pm) found between atoms O8 and O9 reveals the existence of an intramolecular hydrogen bridge between a 2-propanol molecule and a neighboring $\mu_2\text{-(O,O')-bph}$ bridge. In the solid state these ladder-like hexamers form van der Waals 1-D chains, which are further associated according to a hexagonal compact packing involving two disordered chloroform molecules per hexamer. This compact packing is probably responsible for the rather low solubility of the crystals in most organic solvents. The computed lattice energy is in full agreement with this experimental finding. The electrostatic balances of the free hexamer $[\text{Ti}_6\text{O}_4(\text{OPr}^i)_4(\text{PrOH})_2(\text{bph})_6]$ ($Q = +0.76$) and chloroform molecules ($Q = -0.38$) in this system were found to be $\text{EB}_{\text{hexa}} = -19039.0 \text{ kJ}\cdot\text{mol}^{-1}$ and $\text{EB}_{\text{CHCl}_3} = -8.8 \text{ kJ}\cdot\text{mol}^{-1}$. Similar calculations for the full network ($Z = 2$) lead to $\text{EB}_{\text{net}} = -38399.3 \text{ kJ}\cdot\text{mol}^{-1}$, pointing to a rather strong lattice energy, $E_{\text{latt}} = 2(\text{EB}_{\text{hexa}} + 2\text{EB}_{\text{CHCl}_3}) - \text{EB}_{\text{net}} = -286.1 \text{ kJ}\cdot\text{mol}^{-1}$. This value is well in line with the rather high polarity of the individual building blocks which are associated into a network. Owing to this intrinsic low solubility, it was difficult to record good-quality ^1H and ^{13}C NMR spectra in solution. However, we have been able to detect by ^{13}C NMR four signals characteristic of

(23) Crystal data for **4**: $\text{Cl}_6\text{C}_{92}\text{H}_{92}\text{O}_{22}\text{Ti}_6$, $M_r = 2049.86$, monoclinic, space group $P2_1/n$, $a = 13.9560(4) \text{ \AA}$, $b = 20.7380(7) \text{ \AA}$, $c = 16.1330(5) \text{ \AA}$, $\beta = 97.639(3)^\circ$, $V = 4627.8(5) \text{ \AA}^3$, $Z = 2$, $\rho_{\text{calcd}} = 1.47 \text{ g}\cdot\text{cm}^{-3}$, MoK α radiation (graphite monochromator), $\mu = 0.737 \text{ mm}^{-1}$, 28832 intensity data collected at 173 K, 13040 unique, no absorption correction. The structure was solved using direct methods and refined against $|F|$ [7981 reflections having $I > 3\sigma(I)$]. Hydrogen atoms were introduced as fixed contributors when a residual electronic density was observed near their expected positions. For all computations the Nonius OpenMoleN package was used. Refinement converged at $R_1 = 0.064$, $wR_2 = 0.078$, final GOF = 1.323. Residual electron density was in the range $-0.144, 1.622 \text{ e}\cdot\text{\AA}^{-1}$.

(24) Clegg, W.; Elsegood, M. R. J.; Teat, S. J.; Redshaw, C.; Gibson, V. C. *J. Chem. Soc., Dalton Trans.* **1998**, 3037–3039.

(25) (a) Ainscough, E. W.; Brodie, A. M.; McLachlan, S. J.; Brown, K. L. *J. Chem. Soc., Dalton Trans.* **1983**, 1385–1389. (b) Bashkin, J. S.; Schake, A. R.; Vincent, J. B.; Chang, H.-R.; Qiaoying Li, Huffman, J. C.; Christou, G.; Hendrickson, D. N. *J. Chem. Soc., Chem. Commun.* **1988**, 700–702.

the 2,2'-biphenol aromatic rings (CC_2H sites). The absence of the two other signals at 124.8 (CC_3 site) and 152.4 ppm (CC_2O site), easily detected for the free molecule owing to the proximity of the OH group, is strong evidence in favor of the ligands remaining bonded to titanium in solution. The failure to detect other ^{13}C resonances in the aromatic region may then point to a fast exchange between $\mu_2\text{-(O,O')}$ and $\mu_2\text{-(O,O,O')}$ ligands on the NMR time scale.

Conclusion

In summary, we have been able to investigate the coordination modes of aromatic ligands able to form five- (pyrocatechol), six- (salicylic acid), or seven-membered (2,2'-biphenol) chelate rings with Ti(IV) atoms. Three new complexes have been obtained, which have been fully characterized by single-crystal X-ray crystallography. Furthermore, these three complexes have provided us with three different kinds of molecular interactions in the solid state: weak van der Waals (pyrocatechol), hydrogen-bonding (salicylic acid), and polar interactions (biphenol). In each case, we have confirmed our ability to get a good quantitative picture of these rather different intermolecular interactions through the use of partial charge distributions. Owing to the importance of these titanium aryloxides in many fields of chemistry (homogeneous or heterogeneous catalysis, rational design of supramolecular clusters or of metal–organic networks, solar-energy conversion, etc.), work is currently in progress to characterize the chemical reactivity of these new complexes in order to use them as building units in metal–organic networks or as precursors of new hybrid organic–inorganic materials. Work is also in progress to investigate a much wider range of hydrogen-bonded systems, as a quantitative treatment of this fundamental interaction would be of considerable interest not only in chemistry but also in biology and geology.

Acknowledgment. The help of Dr. A. de Cian and Mrs. N. Gruber-Kiritsakas with the X-ray structure analysis is gratefully acknowledged.

Supporting Information Available: Experimental details, including synthesis conditions and spectroscopic characterization of compounds, and a listing of all computed partial charge distributions used in this work and produced by the WinPacha V2.3 software after input of the structural data (PDF); crystallographic files for compounds **1**, **3**, and **4** (CIF). This material is available free of charge via the Internet at <http://pubs.acs.org>.

JA016930F